phys. stat. sol. (c) **2**, No. 7, 2774–2778 (2005) / **DOI** 10.1002/pssc.200461509

Raman, photoluminescence and absorption studies on high quality AlN single crystals

J. Senawiratne[1*], M. Strassburg[1], N. Dietz[1], U. Haboeck[2], A. Hoffmann[2], V. Noveski[3], R. Dalmau[3], R. Schlesser[3], and Z. Sitar[3]

[1] Department of Physics and Astronomy, Georgia State University, Atlanta, GA 30303-3083, USA
[2] Institute of Solid State Physics, Technical University of Berlin, 10623 Berlin, Germany
[3] Department of Material Science and Engineering, North Carolina State University, Raleigh, NC 27695-7919, USA

Received 12 July 2004, revised 16 August 2004, accepted 20 February 2005
Published online 1 April 2005

PACS 78.20.Ci, 78.30.Fs, 78.40.Fy, 78.55.Cr

High quality AlN single crystals grown by physical vapour transport and by sublimation of AlN powder were investigated by Raman, photoluminescence (PL) and absorption spectroscopy. Absorption edges of the AlN single crystals varying from 4.1 eV to 5.9 eV as determined by transmission measurements. Near band edge absorption, PL and glow discharge mass spectroscopy identified impurities such as oxygen, silicon, carbon, and boron that contribute to the absorption and emission bands below the bandgap. The absorption coefficients were derived from UV (6 eV) to FIR (60 meV) spectral range. The exact crystal orientation of the samples, and their low carrier density were confirmed by Raman spectroscopy.

© 2005 WILEY-VCH Verlag GmbH & Co. KGaA, Weinheim

1 Introduction

Quality and life-time of high-power and high-frequency electronic devices and deep UV optoelectronic devices based on wide bandgap group III-Nitrides thin films [1, 2] are hampered by thermal and lattice mismatch to the common substrate materials, such as sapphire, silicon or silicon carbide, that induce high densities of crystal defects, mainly dislocations ($\sim 10^8$-$10^{10}/cm^2$) [3, 4]. The use of AlN bulk crystals as substrate material for group III-Nitride based device structures is expected to yield substantially reduced dislocation densities (below $1000/cm^2$) by minimizing the defects from the substrate and by reducing the lattice and thermal mismatch [5–7]. Hence, the growth and optimisation of bulk AlN crystals is of primary importance for the development of group III-N based devices with improved characteristics and extended lifetime.

In this paper, we report the investigation of AlN single crystals by optical and mass spectroscopy. Varying the process conditions led to different levels of impurities in the AlN single crystals. The impact of these impurities and native defects on the optical and crystalline quality of AlN is studied by absorption, luminescence, and Raman spectroscopy.

[*] Corresponding author: e-mail: jsenawiratne1@student.gsu.edu

© 2005 WILEY-VCH Verlag GmbH & Co. KGaA, Weinheim

2 Crystal growth and experimental

The AlN bulk crystals were grown by a physical vapour transport process from AlN powder and ultra-high purity nitrogen gas at growth temperatures of 1800-2400 °C, and pressures of 400-600 Torr. The results of four characteristic samples, labelled A to D, grown at different temperatures, by different reactions procedures and in different crucibles are reported. A detailed description of the growth process is given in [5, 6, 8–10]. A summary of the most important contaminations and their levels in the AlN bulk crystals recorded by glow discharge mass spectroscopy (GDMS) is given in Table 1.

Table 1 Contamination levels of the AlN single crystals determined by glow discharge mass spectroscopy (GDMS). The concentration is given in ppm wt.

Element	Sample A	Sample B	Sample C	Sample D
B	100	28	0.11	0.77
C	≤300	≤160	≤50	≤30
O	≤500	≤1200	≤50	≤400
Si	5.5	130	40	40
Fe	<0.1	2.4	<0.25	<0.05
Cr	1.1	0.3	<0.1	0.35

The crystalline structure and orientation of the AlN crystals were analysed using Raman spectroscopy. The Raman experiment was conducted applying the 632.8 nm line of a HeNe laser in a backscattering geometry using a charged-coupled device (CCD) attached to a single-grating monochromator for signal detection. Transmission measurements were performed from UV (6.46 eV) to FIR (60 meV) range using different light sources (deuterium lamp, Xenon lamp, halogen lamp etc.), detectors such as photomultiplier (PMT, Hamamatsu R955), InGaAs, InSb, HgTe (MCT), and Tryglycine sulfonate (TGS) detectors, beam splitters and edge filters. A more detailed description of the experimental setup is given in [10, 11]. For the PL investigations, the samples were excited by the forth harmonic of Ti:sapphire laser (5.9 eV). The PL emission was detected by a Hamamatsu R 955 PMT attached to 0.25 m monochromator providing a spectral resolution better than 1 nm.

3 Results and discussion

The crystalline properties were analyzed by x-ray diffraction (XRD) and Raman spectroscopy. The exact wurtzite structure and the crystalline orientation were confirmed by x-ray diffraction (XRD) for all samples unless sample C. The top surface of sample C formed an angle of ~12° relative to the (11-20) crystallographic plane of wurtzite AlN. However, XRD analysis showed the single crystalline nature of the sample C, with full-width at half maximum (FWHM) of less than 0.5° on (11-20) rocking curve. Figure 1 shows the Raman spectra of the investigated samples. The E_2(low) mode at 246 cm^{-1}, the A_1(TO) mode at 609 cm^{-1}, the E_2(high) mode at 655 cm^{-1}, the E_1(TO) mode at 668 cm^{-1}, the A_1(LO) at 895 cm^{-1}, and the E_1(LO) mode at 911 cm^{-1} were revealed. The mode energies of all crystals are in good agreement with absorption bands in the FIR and Raman modes published for unstrained AlN [12–16]. Since no LO mode broadening and LPP modes were observed, the carrier concentrations of the samples are below 10^{18} cm^{-3}. The exact crystalline orientations for the all samples except sample C were confirmed by applying the selection rules. According to the orientation of the c-axis in samples, respective geometries were chosen. E.g., for sample A (c-axis in plane), the $x(zz)\underline{x}$ geometry was chosen since in this geometry the A_1(TO) mode and the E_1(TO) mode are allowed while the E_2(high) mode is forbidden.
The strong intensity of the E_1(LO) mode in sample C is remarkable. According to the presence of multiple grains, the laser wavelength and the low absorption in this spectral range, forward and rectangular scattering are enabled giving rise to the observed strong E_1(LO) mode. Moreover, the coexistence of

© 2005 WILEY-VCH Verlag GmbH & Co. KGaA, Weinheim

A_1(TO), E_2(high), E_1(TO), and E_1(LO) modes, which are supposed to appear in different geometries and polarization, only, indicated the inhomogeneous crystal orientation for sample C, in excellent agreement with GDMS and XRD results mentioned above.

The formation of defect states and bands in the bandgap as a function of the growth conditions and contaminations are analyzed by photoluminescence (PL) and PL absorption spectroscopy. A summary of the PL and absorption recorded in the UV and visible spectral range is shown in Fig. 2. According to the applied excitation energy the luminescence above 5.6 eV was not evaluated. A broad luminescence band having energies well below the bandgap was observed in all samples. An emission band around 4.4 eV is resolved. It was found to be dominant in the spectra in sample C and D, which showed reduced optical

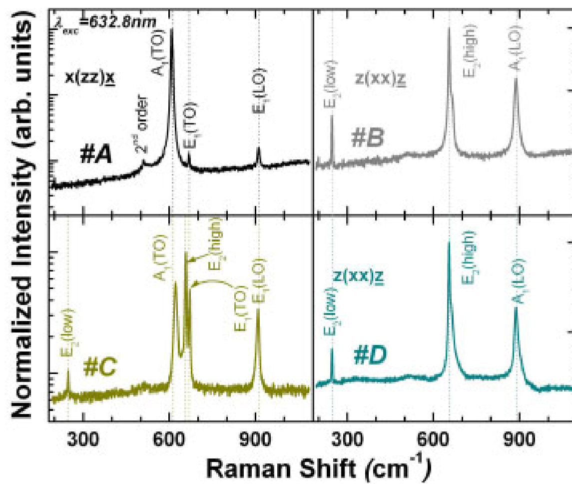

Fig. 1 Raman spectra of the AlN single crystals.

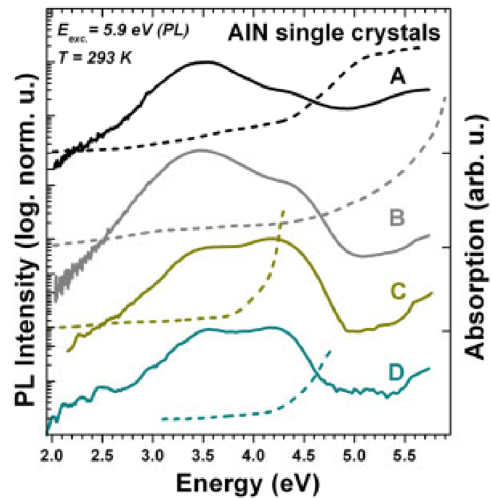

Fig. 2 Photoluminescence (PL) and absorption (dashed lines) of AlN single crystals.

transmission in the UV and the visible spectral range. The PL maximum of the other AlN samples was found to be more redshifted. Defect bands peaking at 3.55 eV and 3.44 eV, respectively, govern the spectra of samples A and B. Based on a fitting procedure with Gaussian curves (not shown here), further peaks of small intensity are determined at 3.93 eV, 4.73 eV and 4.88 eV, being most pronounced in sample A.

The near bandedge transmission facilitates the determination of the absorption edge and hence allows assessment of the optical quality of the crystals. The onset of the transparency for sample B starts at 5.95 eV, while the other crystals become transparent below 4.7 eV (sample A) or even more red-shifted at 4.5 eV (sample D), and 4.1 eV (sample C). The analyzed AlN single crystals exhibited increased absorption at energies approaching the bandgap. In fact, the maximum values of the absorption coefficients, on the order of several hundred cm^{-1}, were located near the bandedge. In the visible and UV range absorption bands were observed at 2.3/2.5 eV, 3.0 eV, and 5.1 eV. However, the absorption decreases in all samples between 4.1 eV and 2.5 eV and remains nearly constant at a minimum value (in the order of a few cm^{-1}) until the IR spectral range (~5 µm), shown in Fig. 3.

© 2005 WILEY-VCH Verlag GmbH & Co. KGaA, Weinheim

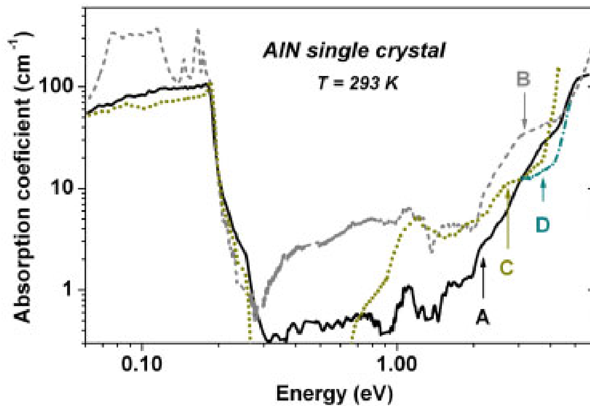

Fig. 3 Absorption coefficient of AlN single crystals from 60 meV to 6 eV.

The comparison of the obtained PL and absorption spectra with the elemental analysis data (GDMS, see Table 1) rules out that oxygen related defects alone are generating the emission band around 3.5 eV. Harris and Youngman [17] found that with increasing oxygen concentration the emission peak energy shifts to lower energies. Despite varying oxygen concentrations (from 50 ppm in sample C up to 1200 ppm in sample B) no significant redshift in the peak energy of the investigated samples was detected. Moreover, the sample with the highest concentration of oxygen (sample B) inherited smallest absorption coefficients in the whole UV spectral range and the highest energy of the absorption edge. Note that a well-defined absorption peak around 4.43 eV, which is in absorption, but not in PL assigned to oxygen related defects, was not detected in sample B. Hence, at least different incorporation sites of oxygen in the samples, but rather other impurities or native defect centers need to be considered as possible culprits for these transitions. GDMS analysis revealed that in addition to O, Si and C were present in the crystals at concentrations that may have a significant influence on the luminescence properties of AlN. In carbon-doped AlN films, C or C-related defect complexes may cause impurity states with respective transition energies around 4.4 eV [18]. However, in this study no straight correlation was detected between the C concentration and the dominance of this PL peak.

An additional PL peak was observed around 2.95 eV in all crystals. Its intensity is more than one order of magnitude less than the observed PL maximum. These broad emission bands were found to consist of several overlapping peaks between 3.55 eV and 2.7 eV [19–22]. It is speculated here that these bands could be assigned to nitrogen vacancies or interstitial Al (3.55 eV and 3.33 eV). Since an emission around 2.8 eV was observed in all crystals the oxygen contamination is below $6*10^{20}$ cm^{-3}. This conclusion was drawn from a defect equilibrium formulation showing that the concentration of oxygen is inversely related to the concentration of nitrogen vacancies [23]. Based on the growth procedure (Sample B: seeded on AlN coated SiC), the presence of vacancies and native defects in crystals sampleA and sample B should be somewhat higher than in sample C and sample D (self-seeded growth). However, this could not be resolved unambiguously by the presented study.

Acknowledgements M.S. gratefully acknowledges the fellowship of the Alexander von Humboldt-foundation. The authors are indebted to U. Perera for the support in the FIR absorption experiments. The growth of AlN was funded by the Office of Naval Research through MURI contract N00014-01-1-0716, Dr. C.E.C. Wood contract monitor.

References

[1] B. Monemar, J. Mater. Sci. Mater. Electron. **10**, 227-254 (1999).
[2] S. Strite and H. Morkoc, J. Vac. Sci. Technol. B **10**, 1237-1265 (1992).
[3] L. Liu and J.H. Edgar, Mater. Sci. Eng. R **37**, 61-127(2002).
[4] O. Ambacher, J. Phys. D: Appl. Phys. **31**, 2653-2710 (1998).

© 2005 WILEY-VCH Verlag GmbH & Co. KGaA, Weinheim

[5] R. Schlesser and Z. Sitar, J. Cryst. Growth **234**, 349-353 (2002).
[6] R. Schlesser, R. Dalmau, and Z. Sitar, J. Cryst. Growth **241**, 416-420 (2002).
[7] J.C. Rojo, G.A. Slack, K. Morgan, B. Raghothamachar, M. Dudley, and L.J. Schowalter, J. Cryst. Growth **231**, 317-321 (2001).
[8] V. Noveski, R. Schlesser, S. Mahajan, S. Beaudoin, and Z. Sitar, J. Cryst. Growth **264** 369(2004).
[9] V. Noveski, R. Schlesser, J. A. Freitas Jr., S. Mahajan, S. Beaudoin, and Z. Sitar, Mater. Res. Soc. Symp. Proc. **798**, Y.2.8 (2004).
[10] M. Strassburg, J. Senawiratne, N. Dietz, U. Haboeck, A. Hoffmann, V. Noveski, R. Dalmau, R. Schlesser, and Z. Sitar, J. Appl. Phys., accepted for publication, scheduled 01. Nov. 2004 (2004).
[11] D.G. Esaev, S.G. Matsik, M.B.M. Rinzan, A.G. Perera, H.C. Liu, and M Buchanan, J. Appl. Phys. **93**, 1879-1883 (2003).
[12] L. Filippidis, H. Siegle, A. Hoffmann, C. Thomsen, K. Karch, and F. Bechstedt, phys. stat. sol. (b) **198**, 621 (1996).
[13] K. Karch, J.-M. Wagner, and F. Bechstedt, Phys. Rev. B **57**, 7043 (1998).
[14] V.Yu. Davydov, Yu.E. Kitaev, I.N. Goncharuk, A.N. Smirnov, J. Graul, O. Semchinova, D. Uffmann, M.B. Smirnov, A.P. Mirgorodsky, and R.A. Evarestov, Phys. Rev. B **58**, 12899 (1998).
[15] R.A. Youngman and J.H. Harris
[16] U. Haboeck, H. Siegle, A. Hoffmann, and C. Thomsen, phys. stat. sol. **0**, 1710-1731 (2003), and references therein.
[17] R.A. Youngman and J.H. Harris, J. Am. Ceram. Soc. **34**, 3228 (1990).; J. H. Harris and R. A. Youngman, in: Properties of Group III Nitrides IEE, EMIS Datarev Series No. 11, edited by J. H. Edgar (Inspec, London, 1994), p. 203.
[18] X. Jiang, F. Hossain, K. Wongchotigul, and M. G. Spencer, Appl. Phys. Lett. **72**, 1501 (1998).
[19] M. Morita, K. Tsubouchi, and N. Mikoshiba, Jpn. J. Appl. Phys., Part 1, **21**, 1102 (1982).
[20] W. M. Jadwisienczak, H. J. Lozykowski, I. Berishev, A. Bensaoula, and I. G. Brown, J. Appl. Phys. **89**, 4384 (2001).
[21] H. Morkoc, Nitride Semiconductors and Devices, edited by R. Hull, R. M. Osgood, Jr., H. Sakaki, and A. Zunger (Springer, New York, 1999), p. 17.
[22] A. Yoshida, Properties, Processing and Applications of Galium Nitride and Related Semiconductors, EMIS Data Reviews Series No. 23, edited by J. H. Edgar, S. Strite, I. Akasaki, H. Amano, and C. Wetzel (London, 1999).
[23] S. Nakahata, K. Sogabe, Y. Matsuura, and Yakahama, J. Am. Ceram. Soc. **80**, 1612 (1997).

© 2005 WILEY-VCH Verlag GmbH & Co. KGaA, Weinheim